Received: 16 September 2019 | Revised: 17 November 2019 | Accepted: 19 November 2019

DOI: 10.1111/jnc.14922

ORIGINAL ARTICLE

Journal of Neurochemistry JNC The Official Journal of the International Society for Neurochemistry WILEY

Metabolic fingerprints discriminating severity of acute ischemia using in vivo high-field ^{1}H magnetic resonance spectroscopy

Mario G. Lepore[1] | Lara Buscemi[2] | Lorenz Hirt[2] | Hongxia Lei[1]

[1]Animal Imaging and Technology Core (AIT), Center for Biomedical Imaging (CIBM), Ecole Polytechnique Fédérale de Lausanne, Lausanne, Switzerland

[2]Centre Hospitalier Universitaire Vaudois (CHUV), Lausanne, Switzerland

Correspondence
Hongxia Lei, EPFL-ENT-R-CIBM-AIT, CH F1 627, Station 6, Lausanne (CH-1015), Switzerland.
Email: hongxiamri@gmail.com

Funding information
The Center for Biomedical Imaging (CIBM) of the UNIL, UNIGE, HUG, CHUV and EPFL, the Leenaards and Jeantet Foundations., Grant/Award Number: N/A

Abstract

Despite the improving imaging techniques, it remains challenging to produce magnetic resonance (MR) imaging fingerprints depicting severity of acute ischemia. The aim of this study was to evaluate the potential of the overall high-field ^{1}H MR Spectroscopy (^{1}H-MRS) neurochemical profile as a metabolic signature for acute ischemia severity in rodent brains. We modeled global ischemia with one-stage 4-vessel-occlusion (4VO) in rats. Vascular structures were assessed immediately by magnetic resonance angiography. The neurochemical responses in the bilateral cortex were measured 1 h after stroke onset by ^{1}H-MRS. Then we used Partial-Least-Squares discriminant analysis on the overall neurochemical profiles to seek metabolic signatures for ischemic severity subgroups. This approach was further tested on neurochemical profiles of mouse striatum 1 h after permanent middle cerebral artery occlusion, where vascular blood flow was monitored by laser Doppler. Magnetic resonance angiography identified successful 4VO from controls and incomplete global ischemia (e.g., 3VO). ^{1}H-MR spectra of rat cortex after 4VO showed a specific metabolic pattern, distinct from that of respective controls and rats with 3VO. Partial-Least-Squares discriminant analysis on the overall neurochemical profiles revealed metabolic signatures of acute ischemia that may be extended to mice after permanent middle cerebral artery occlusion. Fingerprinting severity of acute ischemia using neurochemical information may improve MR diagnosis in stroke patients.

KEYWORDS

acute ischemia, cortex, ^{1}H magnetic resonance spectroscopy biomarker, rodent, striatum

1 | INTRODUCTION

Ischemic stroke is one of the leading causes of death and disability worldwide. Early diagnosis and treatment, especially professional management in the acute phase in specialized stroke units with efficient secondary prevention, have been shown to improve outcome. For instance, cardiac arrest leads to global cerebral ischemia with a poor prognosis if there is not a rapid and successful resuscitation and

Abbreviations used: 3D, three dimension; VO, vessel occlusion; 3VO, occlusion of both carotid arteries and one vertebral artery; 4VO, occlusion of both carotid and vertebral arteries; four-vessel occlusion; pMCAO, permanent middle cerebral artery occlusion; tMCAO, transit middle cerebral artery occlusion; PLS-DA, partial-least-squares discriminant analysis; ^{1}H-MRS, ^{1}H MR Spectroscopy; ^{1}H magnetic resonance spectroscopy; MRA, magnetic resonance angiography; CCA, common carotid artery; VA, vertebral artery; TE, echo time; TE_{eff}, effective echo time; TR, repetition time; GE3D, three dimensional gradient-echo images; SPECIAL, SPin ECho full intensity Acquired Localized; FASTMAP, fast, automatic shimming technique by mapping along projections; BA, basilar artery; LCModel, linear combination of *Model*; Ace, acetate; Ala, alanine; Asc, ascorbate; Asp, aspartate; Cr, creatine; Ins, myo-inositol; GABA, γ-aminobutyric acid; Glc, glucose; Gln, glutamine; Glu, glutamate; Gly, glycine; GPC, glycerol-phosphcholine; GSH, glutathione; Lac, lactate; Mac, macromolecules; NAA, N-acetyl-aspartate; NAAG, N-acetyl-aspartyl-glutamate; PCho, phosphocholine; PCr, phosphocreatine; PE, phosphorylethanolamine; Tau, taurine; CNR, contrast-to-noise ratio; SNR, signal-to-noise ratio; *SD*, standard deviation; MIP, maximum intensity projection; PC, principle component.

spontaneous return of circulation. Thus, early predictors of outcome and response to treatment in experimental models would be very useful both in acute ischemic stroke and/or after cardiac arrest to select and optimize the treatment and management for individual patients. Despite differences among species, thresholds and regions of cerebral ischemia, (Dreher et al., 1998; Hossmann, 1994) the underlying cellular and molecular mechanisms remain substantially common, supporting use of experimental cerebral ischemia models (Traystman, 2003). Amongst these preclinical models, four-vessel occlusion (4VO) is a highly reproducible one that is capable of inducing global ischemia to the entire of forebrain, including bilateral cortex. (Pulsinelli & Brierley, 1979; Sugio, Horigome, Sakaguchi, & Goto, 1988; Yamaguchi, Calvert, Kusaka, & Zhang, 2005) In this model, vessel occlusion is expected to diminish cortical flow,(Kloiber, Miyazawa, Hoehn-Berlage, & Hossmann, 1993; Yamaguchi et al., 2005; Nedergaard, Gjedde, & Diemer, 1986) silence cortical activity,(Horikawa et al., 1985; Kleihues, Hossmann, Pegg, Kobayashi, & Zimmermann, 1975) and immediately deplete ATP and phosphocreatine levels,(Horikawa et al., 1985; Kloiber et al., 1993) while instantly increasing lactate levels. (Behar, Rothman, & Hossmann, 1989; Nagatomo, Wick, Prielmeier, & Frahm, 1995; Taylor, Zhu, Zhang, & Chen, 2015) Since 4VO(Traystman, 2003) can provide the complete acute ischemia condition in the cortex, and most importantly can be performed in the MR scanner as well, (Behar et al., 1989; Taylor et al., 2015) studying metabolic responses of the cortex to acute ischemia and to applicable therapeutic treatments including but not limited to the restoration of blood flow becomes feasible and thus may shed additional insights toward stroke managements.

Recently, we demonstrated that short-echo ^{1}H magnetic resonance spectroscopy (^{1}H-MRS), a noninvasive MR technique, enabled following the longitudinal evolution of metabolites in mouse striatum after transient middle cerebral artery occlusion (Lei, Berthet, Hirt, & Gruetter, 2009) and that the obtained metabolic information provided biomarkers to differentiate subtypes of transient ischemic insults (Berthet, Lei, Gruetter, & Hirt, 2011). Furthermore, we showed that metabolites concentration in the ipsilateral striatum in acute ischemia allow to estimate accurately ischemia onset time in mice after permanent MCAO (pMCAO) in absence of the restoration of cerebral blood flow (Berthet et al., 2014). In particular, some metabolic changes were strikingly different in pMCAO from those in transient middle cerebral artery occlusion, for example, depletion of phosphocreatine to elevation of creatine, accompanied by accumulation of γ-amino-butyric acid levels. (Beckmann, Stirnimann, & Bochelen, 1999; Besselmann, Liu, Diedenhofen, Franke, & Hoehn, 2001; Hilger, Niessen, Diedenhofen, Hossmann, & Hoehn, 2002; Okada, Shima, Nishida, & Kagawa, 1998). For instance, γ-amino-butyric acid elevated without any oxygenation as well (Perry, Hansen, & Gandham, 1981).

We hypothesized that regardless of mammalian species and brain regions, such metabolic changes upon permanent ischemia (i.e., without oxygenation) should be applicable for identification of severities of acute ischemia. Thus, we aimed to evaluate the previously underexplored diagnostic potential of short-echo ^{1}H-MRS at 14.1T after global ischemia in the rat cortex induced by 4VO. As MR offers numerous imaging techniques, not only of anatomical structures, diffusivities and perfusion but also of vasculature, for example, MR angiography (MRA) using blood as an endogenous contrast agent(Reese, Bochelen, Sauter, Beckmann, & Rudin, 1999) that is applicable for vascular occlusion,(Beckmann et al., 1999; Debrey et al., 2008; Hilger et al., 2002; Okada et al., 1998) we extended MRA using the same experimental setting as for ^{1}H-MRS to identify vessel occlusions. We further assessed the potential of metabolic fingerprints to identify the severity of acute ischemia using neurochemical profiles of pMCAO in mouse striatum.

2 | METHODS

2.1 | Animals

All experiments were carried out with the approval of the Veterinary Office of the Canton de Vaud, conducted according to the Federal and Local ethical guidelines of Switzerland (Service de la consummation et des affaires vétérinaires) under license VD2652 (rats) and VD2017.3 (mice), and have been reported following/in compliance with the ARRIVE guidelines for how to report animal experiments. All animals were directly from the vendors and had been rested for at least one week. They were housed in the animal facility with controlled temperature (18–22°C) and humidity (50%–56%) and free access to food and water under a 12-h reverse light-dark cycle (light off at 19:00). Then rats and mice were arbitrarily prepared between 8 h and 15 h.

2.2 | Wistar rats

Sixteen adult male Wistar rats (RGD_13508588, 350–400 g, Charles River, France) were studied in the following three investigated groups. Amongst, eleven rats were udergone the one-stage anterior approach. (Yamaguchi et al., 2005). In brief, all rats were induced anesthesia under 4% isoflurane and kept under 2.5% isoflurane (ATCvet Code: QN01AB06, Attane™, Piramal Enterprises Limited, India) in air/oxygen (1:1) anesthesia. Eleven rats were then placed in a supine position for 4VO and 3VO. After making a 2.5-cm midline skin incision on the neck, subcutaneous connective tissue and muscles were gently retracted to expose cervical vertebral bodies. For 4VO, both vertebral arteries (VAs) were carefully cauterized between cervical diapophysis C2 and C3 using a high temperature cautery pen (Bovie Medical Cooperation). Then, common carotid arteries (CCAs) were carefully isolated and encircled with two inflatable vascular occluders (18080–03, Fine Science Tools, GmbH, Heidelberg, Germany). Once both occluders were inflated completely, 4VO could be achieved. Since 4VO may increase mortality, the number of rats used for this group was increased to seven without any other replacement. Amongst, two rats died immediately after the 4VO and thus were not measured. To obtain incomplete global ischemia (e.g., 3VO), four rats were prepared similarly to 4VO except cauterizing one

VA only. Since such one-stage anterior model does not require any extra days to recover from occluding VA(s) as the standard 4VO(Yamaguchi et al., 2005) and given the aim of this study was to compare with an incomplete ischemia, that is, 3VO, and healthy subjects, five rats not undergoing any vasculature surgery were used as non-surgical controls. To determine the occlusion outcomes, vasculature preparation was blinded to the MR examiner and vasculatures were then imaged and evaluated as described in the following "MR imaging and spectroscopy" session. All other rats were measured, kept anesthetized under isoflurane and then given a lethal dosage of pentobarbital (< 200 mg/ml, 100–150 mg/kg i.p.) for sacrificing after ^{1}H MRS. All rats were given s.c. administration 0.05 mg/kg buprenorphine during surgery to reduce pain throughout the entire of study. A typical summary of rat usages and the experimental layout were shown in Figure 1 a and b.

Given the difference between 4VO and other two groups in selected metabolites may beyond 100%, the number of animals here are sufficient to attain statistical significance of $p < .01$ with a 95% probability when assuming a 20% variation for each mean value (Berthet et al., 2014).

(a)

Species	Strain	Group
Rat	Wistar	4VO ($n = 7$)
Rat	Wistar	3VO ($n = 4$)
Rat	Wistar	Control ($n = 5$)
Mouse*	ICR-CD1	pMCAO ($n = 5$)
Mouse*	ICR-CD1	Sham ($n = 8$)

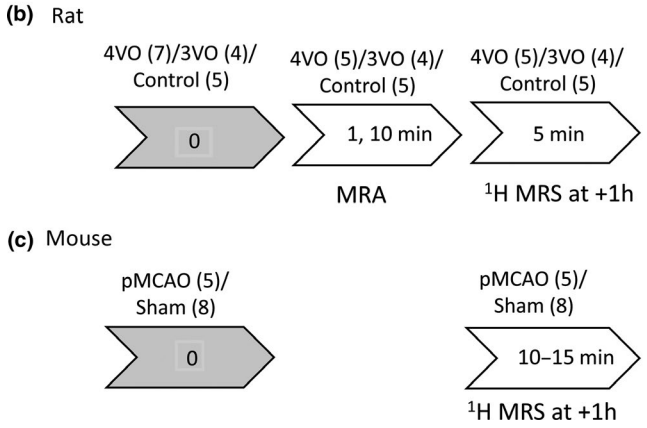

FIGURE 1 Summary of all used animals (a) and typical schematic outlines of rats (b) and mice (c). Mice data were taken from our previous published results (Berthet et al., 2014), indicated with "*". Two rats died after 4VO and were not measured. Mice with blood flow dropped below 20% of the baseline were included (Berthet et al., 2014). The number of rats measured by MRA and ^{1}H MRS and the number of mice used for further analysis are listed in parenthesis (b and c). The duration of the corresponding MR measurements (below the arrows) were listed in the arrows. Abbreviations: MRA, magnetic resonance angiography; ^{1}H MRS, proton magnetic resonance spectroscopy; VO, vessel occlusion; pMCAO, permanent middle cerebral artery occlusion

2.3 | ICR-CD1 mice

The mice results at 1h after another acute ischemia model were taken from our published data (Berthet et al., 2014). In brief, male ICR-CD1 mice (MGI:5,649,797, 20-33g, Charles River, France) underwent pMCAO ($n = 5$) using a filament technique and sham operated procedures without any vasculature operation ($n = 8$). Specifically, mice were anesthetized and maintained under 1.5%–2% isoflurane mixed with 30% oxygen and 70% nitrous oxide. At 0 h, permanent ischemia was induced by inserting a silicone-coated nylon filament (0.17-mm-diameter, 7–0 Superfine MCAO suture, Doccol Co., MA, USA), through the left common carotid artery into the internal carotid artery. Throughout surgery and until awakening, the blood flow was monitored with laser Doppler flowmetry (Periflux 4001 and PROBE 418, Perimed Inc., Sweden) and the rectal temperature of the animal was maintained at 37 ± 0.5°C. Ischemia induction was considered successful if the blood flow dropped below 20% of the baseline. The summary of mouse usages and the experimental layout are shown in Figure 1 a and c. All mice were given s.c. administration 0.05 mg/kg buprenorphine during surgery to reduce pain throughout the entire of study. All mice were sacrificed as rats except with or without isoflurane anesthesia when the designed experiments finished (Berthet et al., 2014). As previously described, 40 mice were used for the previously published study (Berthet et al., 2014). Four mice died and were not measured. Four others were measured but excluded because of (1) the loss of Doppler monitoring signals during the ischemia period, (2) absence of elevated creatine levels within 1 h of ischemia onset, or (3) no ischemic lesion detected by T_2-weighted magnetic resonance imaging at 24 h.

2.4 | Physiological monitoring rats and mice during the MR scan

The animal's head was secured in a horizontal plane with two ear-pieces and a bite bar, cornea protection with gel (VITA-POS, Pharma Medica AG, Switzerland) was applied and fixations into a specific holder for MR experiments. All animals were carefully placed in the center of the MR scanner. Throughout the MR scan we monitored breathing rates (i.e., 50–60 breaths-per-minute for rats and 80–100 breaths-per-minutes for mice, respectively) with an MR compatible system (SA Instrument Inc., USA) and adjusted the delivery concentration of isoflurane in the range of 1%–2%. Body temperature was monitored by a rectal probe and maintained at 36.5–38°C via circulating warm water.

2.4.1 | MR imaging and spectroscopy

All MR studies were performed in a horizontal 14.1-T magnet (260 mm bore, Magnex Scientific Inc.), equipped with a 12-cm inner-diameter gradient (400 mT/m in 200 μs) and interfaced with a Direct-Drive console (Vnmrj, Agilent Inc.). A home-built quadrature surface radio frequency (RF) coil (two geometry decoupled 17-mm-inner-diameter silver-plated copper loops, 0.79 mm^2,

Kabeltronik®, Arthur Volland GmbH, Denkendorf, Germany) covering the entire region of interest was placed on top of the rat's head. In addition, we attached a reference tube containing 10 mM $MnCl_2$ (CAS7773-01–5, Sigma-Aldrich Chemie GmbH, Buchs, Switzerland) to the surface coil and its final position was on the animal's left side.

We used magnetic resonance angiography (MRA) to determine successful vascular occlusion (Beckmann et al., 1999; Debrey et al., 2008; Hilger et al., 2002; Reese et al., 1999). First, we adjusted field inhomogeneity for three dimensional (3D) gradient-echo sagittal images (GE3D, echo-time (TE)/repetition-time (TR) = 1.5/6 ms, field-of-view = 35 × 35 × 45 mm^3, phase-encode × phase-encode 2 × readout=96 × 96 × 160, spectral-width = 100 kHz). To determine the complete CCAs, GE3D was applied with only one average immediately after the occlusion. In order to generate maximum intensity projection (MIP) images (Hilger et al., 2002; Reese et al., 1999) of both CCAs and VAs with a satisfactory signal-to-noise ratio (SNR), flip angles were set at 90° for GE3D with 8 averages to sufficiently minimize stationary MR signals from tissues while non-stationary MR signals originated from arterial bloods were enhanced.

For metabolic signatures (fingerprints) of ischemic severity (described later), we used high-field ^{1}H-MRS as previously applied in mice (Berthet et al., 2011, 2014; Lei et al., 2009). In this study, once the bilateral cortical tissue (34–45 µl, e.g., 8 × 1 × 4.5 mm^3) was defined based on T_2-weighted anatomical images (fast spin echo image, $TE_{effective}$/TR = 50/4000 ms, 8 averages) and field inhomogeneity was improved by the Fast, Automatic Shimming Technique by Mapping Along Projections (FASTMAP), (Gruetter & Tkac, 2000) we acquired localized short-echo ^{1}H MR spectra (TE/TR = 2.8/4000 ms, 80 averages, SPin ECho, full intensity Acquired Localized, SPECIAL(Mlynarik, Gambarota, Frenkel, & Gruetter, 2006)) from bilateral cortex with sufficient water suppression approximately 1 h after CCA occlusion (Behar et al., 1989; Berthet et al., 2014). Resulting SNRs were ensured to be >15. Immediately after, water signal from the identical volume was acquired (TE/TR = 2.8/4000 ms, 8 averages).

We assured similar spectral quality and SNRs in mice, as described previously. (Berthet et al., 2014) For instance, we applied increasing number of averages (160–240) on the ipsilateral striatum (6–8 µl, e.g., 2 × 1.6 × 2 mm^3) to reach sufficient SNR.

2.5 | Data analysis and statistics

The maximum intensity projection (MIP) images were generated from the GE3D volume images. Since one VA was occluded for the anticipated 3VO, the resulting MR images were then processed pixel-per-pixel to obtain contrast-to-noise (CNR) values between signals from the reference tube containing 10mM $MnCl_2$ and signals from the basilar artery (BA).

All ^{1}H-MR spectra were collected, processed offline and then quantified using the LCModel (Linear Combination Model, LCModel2013) algorithm using the endogenous water signal from the identical volume (i.e., 80% of water content stands for a 44.4 mol/L concentration), as previously (Lei et al., 2009). In particular, acetate (Ace), alanine (Ala), ascorbate (Asc), aspartate (Asp), creatine (Cr), myo-inositol (myo-Ins), -aminobutyric acid (GABA), glucose (Glc), glutamine (Gln), glutamate (Glu), glycine (Gly), glycerol-phosphcholine (GPC), glutathione (GSH), lactate (Lac), macromolecules (Mac), N-acetyl-aspartate (NAA), N-acetyl-aspartyl-glutamate (NAAG), phosphocholine (PCho), phosphocreatine (PCr), phosphorylethanolamine (PE), and taurine (Tau) were included in the basis set of the LCModel. All of these metabolites except Ace were quantified with desired SNRs (e.g., >10) with Cramér–Rao lower bounds (CRLBs) less than 35% in healthy rats and mice. After global ischemia, some metabolites were expected to be reduced to very low levels and remained to be reported, such as glucose (Glc) and phosphocreatine (PCr) (Berthet et al., 2014). Although the only strong correlation between GPC and PCho at 9.4T, that is, >0.5 (Tkac et al., 2004), reduced substantially at 14.1T (Mlynarik et al., 2006), the sum of GPC and PCho (GPC + PCho) was used for further analysis.

We carried out statistical tests on all measured data of rat cortex and the previously published data of mouse striatum(Berthet et al., 2014) using GraphPad (Prism5, STATCON, Germany) without either assessment of the normality of data or any outliers, and then we used two-way ANOVA with Bonferroni *post-hoc* correction unless stated otherwise. Values were shown as mean ± standard deviations (*SD*s) and a significant level was reached when *p*-value was ≤0.05. When multiple comparisons were made, the correction was applied.

2.5.1 | Characterization of metabolic signatures of acute ischemia using partial least squares discriminant analysis on the overall neurochemical profile

The partial least squares discriminant analysis (PLS-DA) has been shown capable of seeking a decision function based on a large number of metabolites for a clear separation of different groups,(Lei et al., 2019) and provides insight into seeking how much each metabolite contributes to the causes of discrimination via its specific weights and loadings (Brereton & Lloyd, 2014). Thus, we applied this approach (MetaboAnalyst4.0) (Xia & Wishart, 2016) on the overall metabolite concentrations (i.e., neurochemical profile) of rat cortex to evaluate the corresponding weights and loadings of each component (i.e., principle component, PC) influencing the final PLS-DA outcomes (i.e., score plots) and thus to produce metabolic fingerprints indicating severity of acute ischemia.

To further test this approach, we included data from a previous study of our laboratory using another acute ischemia model, pMCAO in the mouse,(Berthet et al., 2014) from which we took mice measured 1 h after ischemic onset and their respective controls.

3 | RESULTS

3.1 | Magnetic Resonance Angiography (MRA) and high-field ^{1}H-MRS identified rats undergoing global ischemia

After suppressing stationary tissue signals, MRA showed both the brain supplying arteries and the intracranial arteries in control rats (Figure 2a) along with the reference signal (SNR = 572 ± 34). While in 4VO rats there was no signal neither in brain supplying arteries nor in intracranial arteries, the MRA in 3VO showed 1 patent vertebral artery supplying the basilar artery and the arterial circle. The quality MIP images of the 4VO rats displayed diminished vascular signals (8 averages, Figure 2). Consequently, the contrast from the MR signal of the reference versus that of BA, that is, 478 ± 4, was the highest when compared to that of matched controls (277 ± 21, unpaired *t*-test *p*-value < 0.05) and that of the 3VO rats (434 ± 8, *p*-value <0.05).

The typical ^{1}H MR spectra of the rat cortex shown in Figure 2 depict abundant metabolites in controls (metabolic linewidths 13 ± 1.7 Hz), with apparent changes after 4VO (metabolic linewidths 17 ± 2.6 Hz), namely increased Lac and GABA peaks, (Figure 3b). Further analysis revealed other metabolic changes in the 4VO rats compared to respective controls (Figure 3), notably in energy related substrates (e.g., Cr, Glc, and PCr) as well as neurotransmitters (e.g., GABA and Gln + Glu). In the 3VO rats, levels of most metabolites were similar to those of healthy controls (Figure 3c) except for some slight increases in Glc and Lac. In addition, Cr increased slightly and consequently led to a lower PCr/Cr in 3VO rats (0.8 ± 0.2) than that of controls (1.2 ± 0.2, *p*-value < 0.05).

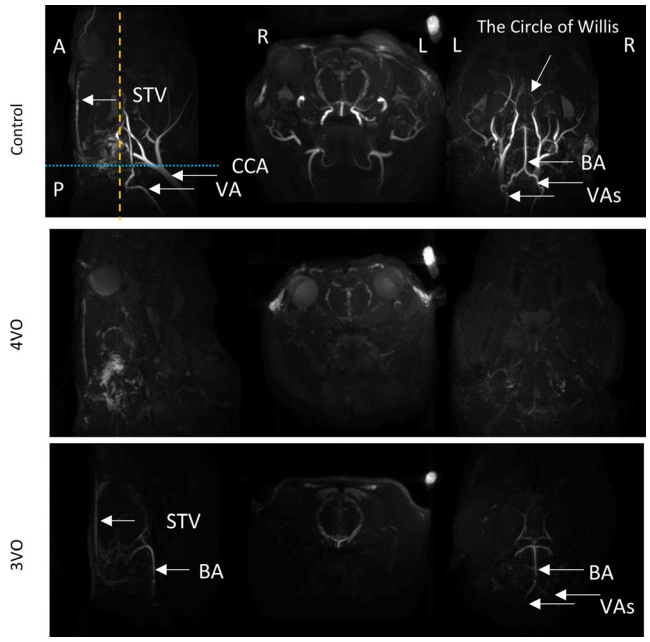

FIGURE 2 Representative maximum intensity projection (MIP) maps showing major head vessels in healthy control rats, but limited MIP signal from vessels after 3VO and 4VO. All maps are displayed in sagittal (at the midline of the brain), coronal (blue dotted line), and axial (orange dashed line) planes. The Circle of Willis (BA toward the anterior part of the head) can be visualized in both healthy and 3VO rats. The bright round spots are signals from a reference tube containing 10 mM $MnCl_2$, attached to the surface coil and its final position was on the animal's left side. In order to illustrate the residues of the MIP signal intensities in 4VO, the reference signal was displayed with slightly amplified amplitudes. Abbreviations: BA, basilar artery; VA, vertebral artery; CCA, common carotid artery; STV, superficial temporal vein. Orientation: A, anterior; P, posterior; R, animal's right; L, animal's left

3.2 | High-field ^{1}H-MRS discerned degrees of acute ischemia in rats and mice

We used PLS-DA to take advantage of the overall neurochemical profiles of cortex for discerning the three investigated groups, that is, the 4VO, 3VO, and control rats, by evaluating the corresponding weights and loadings of each neurochemical component. Scatter plots of PLS-DA score outcomes of the corresponding neurochemical profiles clearly separated the 4VO rats from controls and 3VO rats with principal components 1 and 2 (PC1 and PC2, Figure 4 a); the separation into three groups is even clearer when using PC1 and PC3 (Figure 4b). It is of interest to note that the contributing weights of some metabolites are altered in PC3 with respect to PC2, for example, Lac, as shown in the corresponding loading factors (Figure 4c).

We further tested this approach of evaluating the overall neurochemical profiles to identify metabolic signatures specific to acute ischemia on another acute stroke model, namely pMCAO with ipsilateral striatal ischemia in mice, published previously (Berthet et al., 2014). Taking the neurochemical profiles of ipsilateral striatum of five mice 1h after pMCAO and those of eight controls provided a clear separation between pMCAO and controls as shown in Figure 5. Notably, the strikingly different amplitudes of metabolite changes, for example, Lac, (Figure 6) were adjusted accordingly.

4 | DISCUSSION

In this study, we showed that it is feasible to validate complete 4VO in rats using MRA technique with the identical experimental settings for ^{1}H MRS. Moreover short-echo localized ^{1}H MRS identifies the metabolic consequences in the bilateral cortex after such severe acute ischemia relative to healthy cortex. Notably, ^{1}H-MRS metabolic 'patterns' reflect the severity of the ischemia. To show relevance of the methodology we demonstrate that the characteristic metabolic signatures of acute ischemia are applicable to another rodent model of acute ischemia. The distinct neurochemical consequences of acute ischemia therefore open the possibility to fingerprint acute stroke severity and thus to improve stroke diagnosis.

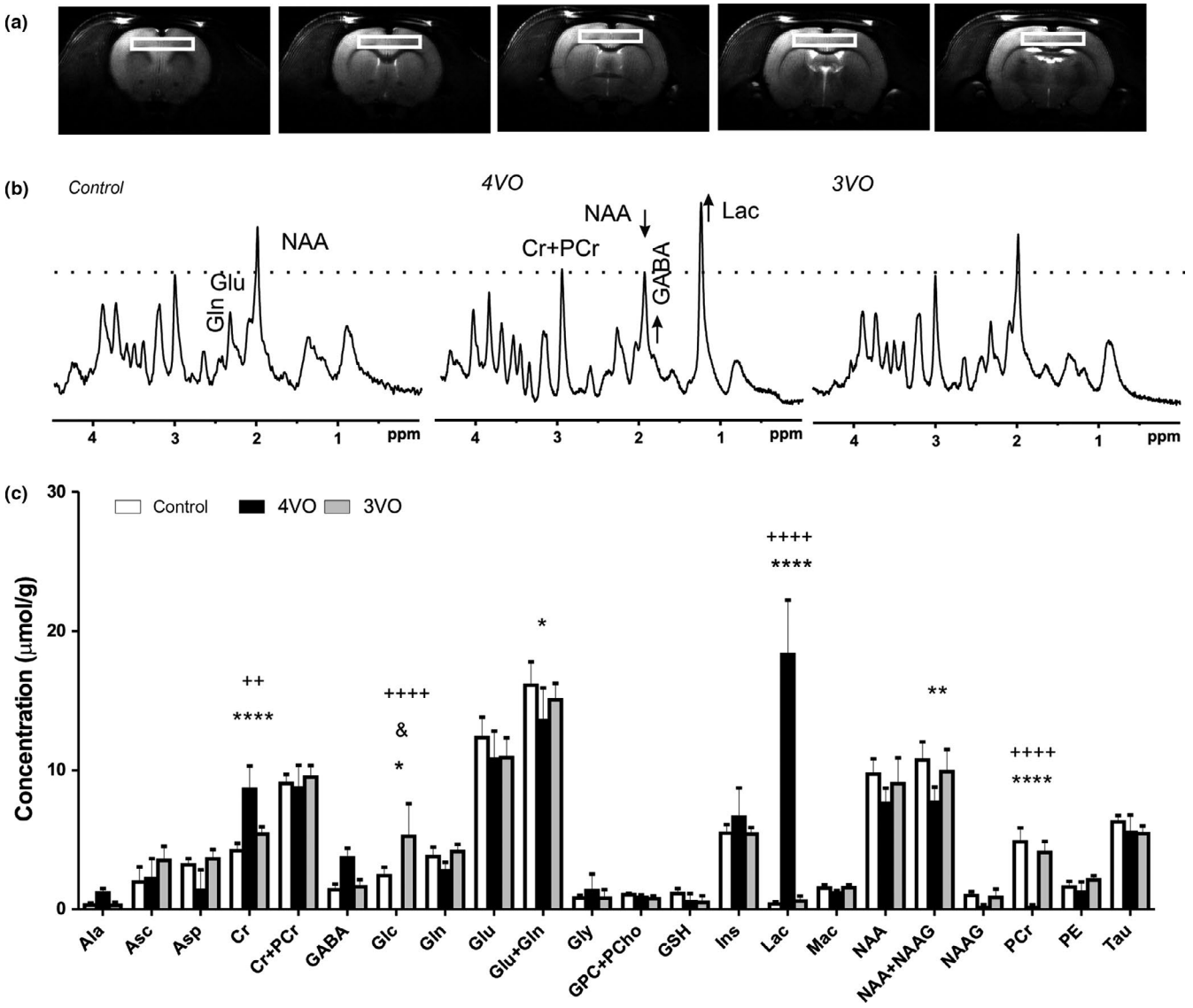

FIGURE 3 Localized ^{1}H MR Spectra (b) and neurochemical profiles (c) of the bilateral cortex (e.g., 8 × 1 × 4.5 mm^3, depicted with rectangles in typical consecutive T_2-weighted anatomical MR images, a) from the three study groups showed distinct characteristics of 4VO from its respective control and 3VO. In b, visual spectral changes of 4VO compared to control are highlighted (arrows). The dashed line is at the height of the total creatine (Cr + PCr) resonance peak showing that all spectra were normalized to Cr + PCr level using line-broadening apodization. In c, the corresponding neurochemical profiles of control (white bars, n = 5), 3VO (gray bars, n = 4) and 4VO (solid black bars, n = 5) rats are summarized (all individual data were provided in Table S1). Spectral quantification confirmed visual differences between control and 4VO rats (b) with additional metabolic changes, marked as follows: Statistical differences were calculated using two-way ANOVA and followed by the Bonferroni post-tests. "*" indicates 4VO versus control; "+" 4VO versus 3VO; "&" 3VO versus control. Increasing numbers of symbols indicates statistical p-values lower than 0.05, 0.01, and 0.001, respectively. Error bars were *SD*s. Abbreviations: alanine (Ala), ascorbate (Asc), aspartate (Asp), creatine (Cr), myo-inositol (Ins), γ-amino-butyric acid (GABA), glucose (Glc), glutamine (Gln), glutamate (Glu), glycine (Gly), glycerophosphocholine + phosphocholine (GPC + PCho), glutathione (GSH), lactate (Lac), N-acetyl-aspartate (NAA), N-acetyl-aspartyl-glutamate (NAAG), phosphocreatine (PCr), phosphatidylethanolamine (PE), and taurine (Tau)

4.1 | Non-invasive identification of 4VO using MRA and high-field ^{1}H-MRS

MRA has been applied to image vasculatures in standard clinical settings (Debrey et al., 2008). Here we extended the use of a surface coil with an external reference signal showing that vascular intensities could be evaluated accordingly. Vascular intensities were noticeably decreased in rats with both CCAs and one VA occluded (3VO), and were practically abolished in all 4VO rats (Figure 2). The quality of MIP images permitted identification of complete global ischemia in rats using a non-invasive approach for monitoring cortical blood flow (Lei et al., 2009). Furthermore, high-field ^{1}H-MRS on the bilateral cortex of the three investigated groups showed that substantial number of neurochemical changes in cortical tissue (e.g.,

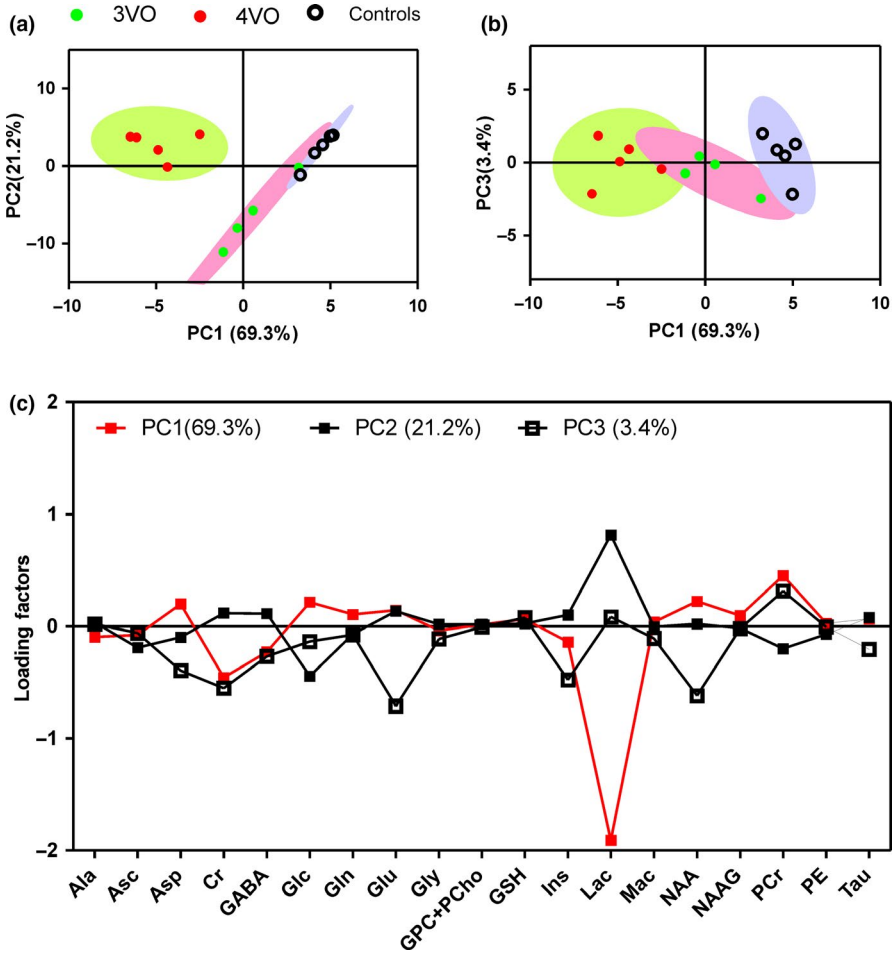

FIGURE 4 Scatter plots (a and b) and their corresponding loading factors (c) of all partial least squares discriminant analysis (PLS-DA) results of controls, 3VO and 4VO rats. In (a), 4VO (solid red dots) clusters distinctly from 3VO (solid green dots) and controls (open black circles) using principal component 1 (PC1) and PC2. In combination with PC3, all three groups were clearly separated, as shown in (b). In (a) and (b), the corresponding 95% confidential ellipses were marked in green for 4VO, pink for 3VO and purple for controls. (c) Evaluation of the corresponding loading factors of the PLS-DA outcomes, with a clear contribution from PC1 (solid red squares) to separating 4VO rats from 3VO and control ones (a); a clear separation of all three groups (b) was achieved by enhancing the contributions of Asp, Cr, GABA, Glu, Ins, NAA and PCr in PC3 (open black squares) while reducing the contributions of Asc, Glc, and Lac (PC2, solid black squares). Abbreviations: alanine (Ala), ascorbate (Asc), aspartate (Asp), creatine (Cr), myo-inositol (Ins), γ-amino-butyric acid (GABA), glucose (Glc), glutamine (Gln), glutamate (Glu), glycine (Gly), glycerophosphocholine + phosphocholine (GPC + PCho), glutathione (GSH), lactate (Lac), N-acetyl-aspartate (NAA), N-acetyl-aspartyl-glutamate (NAAG), phosphocreatine (PCr), phosphatidylethanolamine (PE), and taurine (Tau)

highly elevated Lac) occurred in the case of complete 4VO (Figure 3). For instance, the elevated Lac level after 4VO in rats (i.e., 18.2 ± 3.9 μmol/g) is in excellent agreement with previous observations of acute stroke in the mouse(Berthet et al., 2014), rat (Chang, Shirane, Weinstein, & James, 1990), cat(Behar et al., 1989), and gerbil(Crockard et al., 1987; Gadian et al., 1987). Since high Lac contents in acute stroke have been proposed to induce acidosis (Behar et al., 1989; Chang et al., 1990) and pH change is noticeably associated with Lac concentration in a linear fashion (i.e., pH = −0.0577×[Lac]+7.23, derived from Chang et al. 1990), the pH in our rats after 1 h of ischemia was expected to be 6.17 ± 0.22, assuming pH of controls at 7.1. The resulting pH is in excellent agreement with that of cat cortex after 1 h of global ischemia (Dreher et al. 1998).

4.2 | High-field ^{1}H–MRS revealed distinctive neurochemical profiles of 4VO rats

Additional metabolic alterations occurred after complete global ischemia, including elevation of Cr associated with reduction in PCr (Figure 3c). However, after incomplete global ischemia, 3VO, cortical metabolites remained largely unchanged compared to their respective controls (Figure 3c). However, a significant decrease in PCr/Cr (0.8 vs. 1.2) was noticeable. In addition, Glc increased substantially, which was opposite to its change after 4VO. Therefore, either metabolic adaption or reduced energy expenditure or both might occur in cortex after 3VO, a condition characterized by reduced blood circulation, further confirmed by amplified CNRs between the reference and BA signals (Figure 2). Furthermore, all other energy related substrates

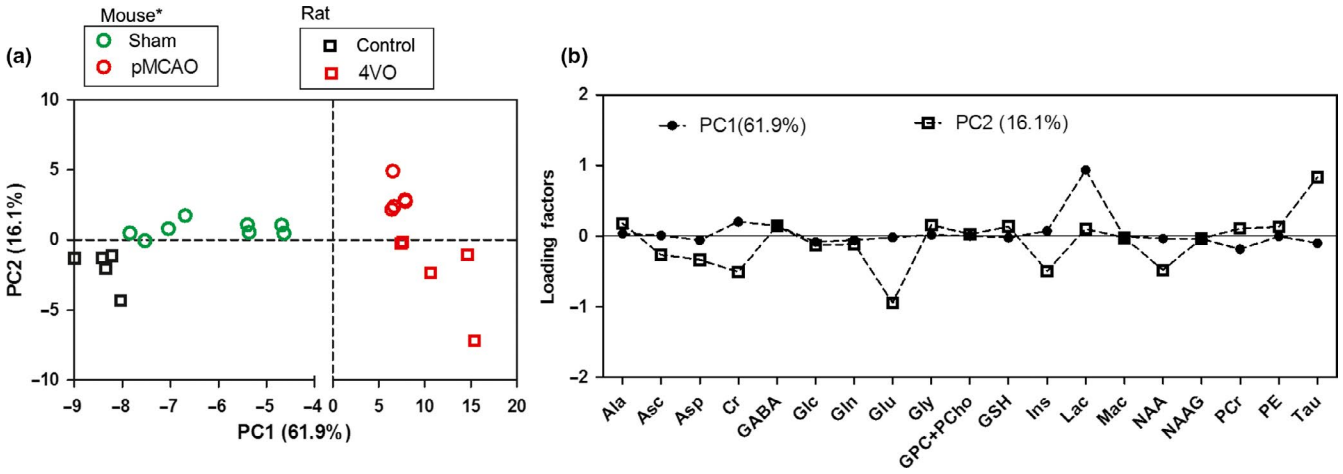

FIGURE 5 Partial least squares discriminant analysis (PLS-DA) of neurochemical profiles separated all acute ischemic animals, including the 4VO rats (red open squares) and pMCAO mice (red open circles), from their respective controls, that is, the control rats (control, black open squares) and the sham-operated mice (sham, green open circles), as shown in (a). The corresponding loading factors (b) indicated individual contribution weight of each metabolite to such clear separation of both ischemia and non-ischemic ones. Noticeably, PC1 is the main component for separation of acute ischemia (both pMCAO and 4VO) from non-ischemic ones (both sham and control). PC2 becomes dominant in the separation of the two acute ischemia models (species, brain regions, and subjects) "*" indicates the data (all individual mouse data were provided in Table S2) were from Berthet et al., (2014). Abbreviations: alanine (Ala), ascorbate (Asc), aspartate (Asp), creatine (Cr), myo-inositol (Ins), γ-amino-butyric acid (GABA), glucose (Glc), glutamine (Gln), glutamate (Glu), glycine (Gly), glycerophosphocholine + phosphocholine (GPC + PCho), glutathione (GSH), lactate (Lac), N-acetyl-aspartate (NAA), N-acetyl-aspartyl-glutamate (NAAG), phosphocreatine (PCr), phosphatidylethanolamine (PE), and taurine (Tau)

of the rat cortex upon 3VO, differed from those after 4VO (Figure 3c). Thus, we suggest that at the analyzed time point, energy sources from the blood stream were sufficient to maintain the existing cortical metabolic demands without substantially altering most of the abundant metabolites, for example, Glu, Gln, and NAA etc (Berthet et al., 2014). Although we cannot exclude any potential effects of an extended length of 3VO (1 h in this study) on other brain regions, for example, dorsal hippocampus, ^{1}H-MR spectra retained sufficient quality for specific metabolic status of such incomplete global ischemia in cortex.

Of note, our experimental setting permits induction of global ischemia as well as reperfusion within the MR scanner, (Behar et al., 1989; Taylor et al., 2015) and consequently allows us to study the cortical metabolic responses immediately after acute ischemia and restoration of blood flow, which remains to be explored further. The model chosen here is extremely severe. Not surprisingly, we observed changes in the 4VO rats similar to those in postmortem rats (Figure S1), in major energy related substrates (e.g., Glc, Lac, Cr, and PCr) and neurotransmitters (e.g., Gln and GABA) but with noticeable minor amplitude differences and some metabolic differences (e.g., Asp and NAA), thereby reinforcing the notion that care should be taken when comparing in vivo ^{1}H-MRS data with biochemical analysis on postmortem models.

4.3 | Metabolic signatures of acute ischemia regardless of species, brain regions, or ischemia types

We took advantage of the PLS-DA on seeking the optimized discriminator based on the large amount of metabolites concentration data to separate clearly the 4VO rats from their respective controls and the incomplete occlusion (3VO) rats as shown in Figure 4. As expected, energy related metabolites, for exmple, PCr, Cr, Lac, and Glc, had large loading values (Figure 4c), which indicated the significant contribution toward fingerprinting the acute ischemia.

Remarkably, our 4VO results show a similar reduction in PCr and increase in lactate levels as cats after identical global ischemia(Behar et al., 1989; Taylor et al., 2015) and mice after pMCAO (Berthet et al., 2014). After pMCAO, despite the fact that there is some residual blood flow in the dorsal striatum(Nedergaard et al., 1986) and several neurochemicals exhibit concentration variations in different rodent brain regions,(Duarte, Lei, Mlynárik, & Gruetter, 2012) the neurochemical consequences in the absence of oxygen remain remarkably similar (Perry et al., 1981). For instance upon acute ischemia (i.e., no oxygenation), anaerobic glycolysis becomes the dominating process and transforms Glc to Lac, thus explains the common observations in our two different acute ischemia models, for example, diminished Glc and accumulated Lac in both ischemic brain tissues (Figure 5). One of key bioenergetics substrates, PCr, reduced to non-detectable levels, which are similar to many previous reported ^{31}P MR studies of ischemia (Horikawa et al., 1985; Kloiber et al., 1993). On top of that, ^{1}H MRS at 14.T also showed capability of detecting the production of depletion of PCr, that is, Cr.,(Lei et al., 2009, 2019; Tkac et al., 2004) which rose sharply upon acute ischemia (Figures 3 and 6). The PCr decline and Cr increase in ischemic brain tissues of two acute ischemia models are consistent with the previously reported immediately deplete ATP upon acute ischemia (Horikawa et al., 1985; Kloiber et al., 1993). Taking together, the energy related substrates in both ischemic brain tissues showed their alterations with the same direction upon acute ischemia but with some amplitude differences

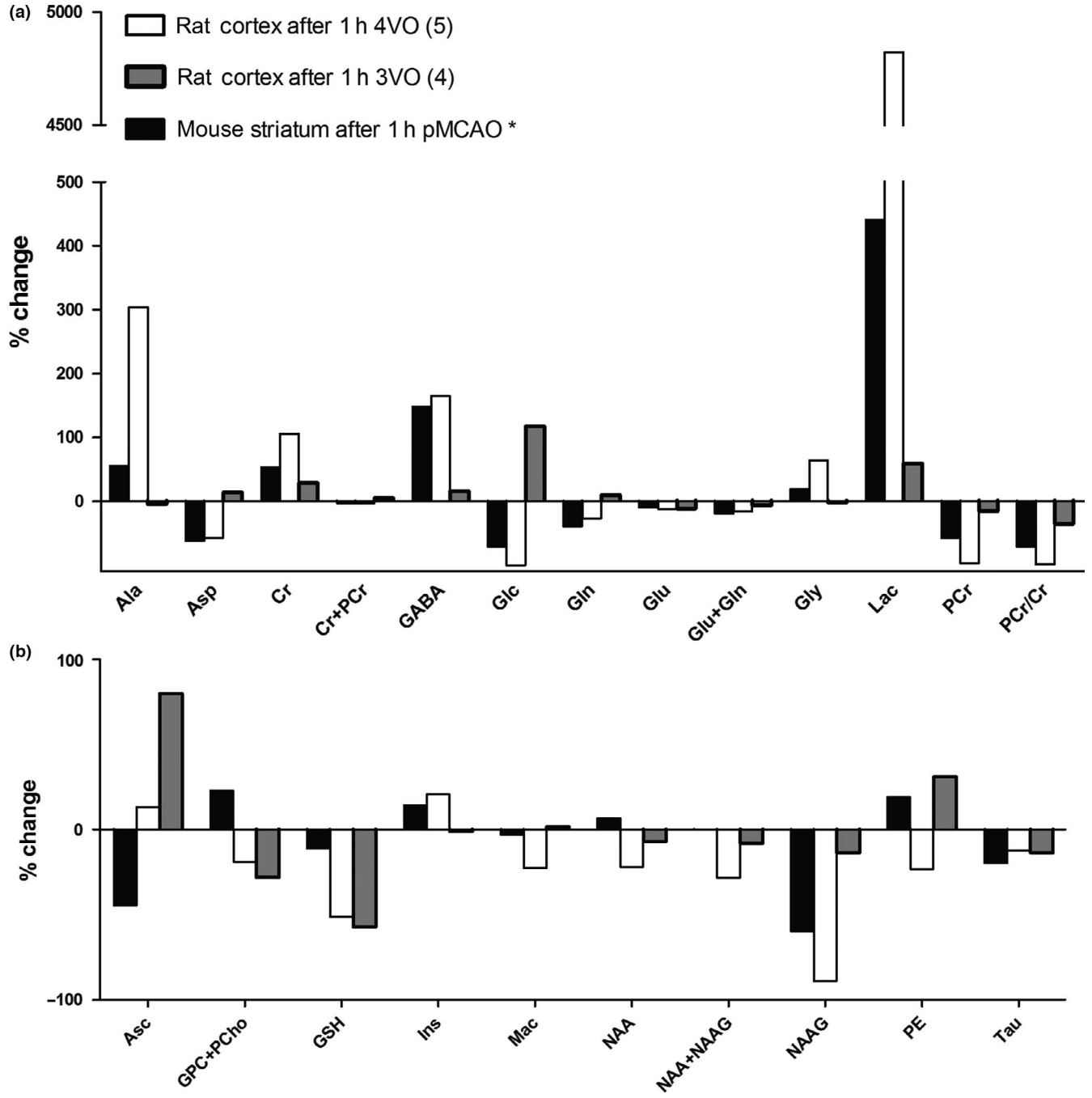

FIGURE 6 Percent changes of neurochemicals in mouse striatum 1 h after pMCAO (Berthet et al., 2014), and rat cortex 1 h after 4VO or 3VO. Some of metabolites were summed and PCr to Cr ratio (PCr/Cr) was also calculated. The reported percent changes were calculated based on their perspective controls, that is, sham-operated animals. Compared to 3VO, most energy-related metabolic changes in both acute ischemic models without perfusion were in the same direction (a) but with different amplitudes. "*" indicates that pMCAO data were taken from Berthet et al., (2014). Abbreviations: alanine (Ala), ascorbate (Asc), aspartate (Asp), creatine (Cr), myo-inositol (Ins), γ-amino-butyric acid (GABA), glucose (Glc), glutamine (Gln), glutamate (Glu), glycine (Gly), glycerophosphocholine + phosphocholine (GPC + PCho), glutathione (GSH), lactate (Lac), N-acetyl-aspartate (NAA), N-acetyl-aspartyl-glutamate (NAAG), phosphocreatine (PCr), phosphatidylethanolamine (PE), and taurine (Tau)

(Figure 6). Furthermore, excitatory (Gln and Asp) and inhibitory neurotransmitters (GABA and Gly) exhibited similar trends due to acute ischemia induced such energy deficit (Figure 6).

With the aim of seeking possible metabolic signatures of ischemic damages from their corresponding controls despite the differences in species, brain regions and models of acute ischemia, the PLS-DA of resulting neurochemical profiles of ischemic brain tissues (both ischemic rat cortex and ipsilateral mouse striatum) clearly allows differentiation from non-ischemic ones (both control rats and sham mice, Figure 5a). Strikingly, some differences in controls

and acute ischemia were clearly noticeable. This is consistent with differences among the ischemic brain region (rat cortex vs. mouse striatum) and the ischemia-induced metabolic amplitude changes (4VO vs. pMCAO), as summarized in Figure 6. For instance, PC1 is responsible not only for separating ischemic and non-ischemic brain tissues but also for normal brain tissues, for example, Lac (Figure 5b). In addition, Cr, Tau, and Glu become additional major contribution factors (e.g., loading factors >0.5) in the PC2 to differentiate ischemic tissues, that is, ischemic rat cortex and ipsilateral mouse striatum, respectively (Figure 5b). This might be explained by specie and region differences.

Furthermore in the mouse pMCAO study, (Berthet et al., 2014) we were able to use the steady declines of Tau, NAA and similarly for the sum of NAA + Tau + Glu to predict ischemia onset time. Taken together, we could potentially use the very time-specific neurochemical responses to permanent ischemia and incomplete vascular occlusion to characterize acute stroke severity, (Berthet et al., 2011, 2014; Djuricic, Paschen, Bosma, & Hossmann, 1983) opening the possibility to fingerprint degree of ischemia and duration. Given human brains present similar metabolic information to rodent brains but different concentrations and the aforementioned metabolites are detectable with the use of robust MRS in the clinical settings, (Fisher, Prichard, & Warach, 1995; Öz et al., 2014) the ^{1}H-MRS neurochemical profile in conjunction with the PLS-DA will provide additional valuable information to clinician about ischemia severity,(Fisher et al., 1995) guiding diagnosis and to some extent helping prognosis.

5 | CONCLUSION

In conclusion, high-field ^{1}H-MRS allows detection of distinct neurochemical responses in the cortex after acute cerebral ischemia resulting either from acute ischemic stroke (focal) or from abolished brain perfusion such as in cardiac arrest (global), and may improve diagnosis by fingerprinting ischemia severity.

ACKNOWLEDGMENTS

This work was supported by the Center for Biomedical Imaging (CIBM) of the UNIL, UNIGE, HUG, CHUV, and EPFL, the Leenaards and Jeantet Foundations. We thank Dr Melanie Price for carefully proofreading the manuscript. Authors declare no potential conflict of interests relevant to this article.

All experiments were conducted in compliance with the ARRIVE guidelines.

AUTHOR CONTRIBUTION

HL contributed to study concept, acquisition and analysis of MR data, and drafting of the manuscript. ML and LB contributed to animal models. HL and LH contributed to interpretation of data. ML, LB, LH, and HL revised the manuscript.

ORCID

Hongxia Lei https://orcid.org/0000-0002-4065-9331

REFERENCES

Beckmann, N., Stirnimann, R., & Bochelen, D. (1999) High-resolution magnetic resonance angiography of the mouse brain: Application to murine focal cerebral ischemia models. *Journal of Magnetic Resonance 140*, 442–450. https://doi.org/10.1006/jmre.1999.1864

Behar, K. L., Rothman, D. L., & Hossmann, K. A. (1989) NMR spectroscopic investigation of the recovery of energy and acid-base homeostasis in the cat brain after prolonged ischemia. *Journal of Cerebral Blood Flow and Metabolism 9*, 655–665. https://doi.org/10.1038/jcbfm.1989.93

Berthet, C., Lei, H., Gruetter, R., & Hirt, L. (2011) Early predictive biomarkers for lesion after transient cerebral ischemia. *Stroke 42*, 799–805. https://doi.org/10.1161/STROKEAHA.110.603647

Berthet, C., Xin, L., Buscemi, L., Benakis, C., Gruetter, R., Hirt, L., & Lei, H. (2014) Non-invasive diagnostic biomarkers for estimating the onset time of permanent cerebral ischemia. *Journal of Cerebral Blood Flow and Metabolism 34*, 1848–1855. https://doi.org/10.1038/jcbfm.2014.155

Besselmann, M., Liu, M., Diedenhofen, M., Franke, C., & Hoehn, M. (2001) MR angiographic investigation of transient focal cerebral ischemia in rat. *NMR in Biomedicine 14*, 289–296. https://doi.org/10.1002/nbm.705

Brereton, R. G., & Lloyd, G. R. (2014) Partial least squares discriminant analysis: Taking the magic away. *Journal of Chemometrics 28*, 213–225.

Chang, L. H., Shirane, R., Weinstein, P. R., & James, T. L. (1990) Cerebral metabolite dynamics during temporary complete ischemia in rats monitored by time-shared ^{1}H and ^{31}P nmr spectroscopy. *Magnetic Resonance in Medicine 13*, 6–13. https://doi.org/10.1002/mrm.1910130103

Crockard, H. A., Gadian, D. G., Frackowiak, R. S., Proctor, E., Allen, K., Williams, S. R., & Russell, R. W. (1987) Acute cerebral ischaemia: Concurrent changes in cerebral blood flow, energy metabolites, pH, and lactate measured with hydrogen clearance and ^{31}P and ^{1}H nuclear magnetic resonance spectroscopy. II. Changes during ischaemia. *Journal of Cerebral Blood Flow and Metabolism 7*, 394–402. https//doi.org/10.1038/jcbfm.1987.82

Debrey, S. M., Yu, H., Lynch, J. K., Lövblad, K.-O., Wright, V. L., Janket, S.-J.- D. and Baird, A. E. (2008) Diagnostic accuracy of magnetic resonance angiography for internal carotid artery disease. *A Systematic Review and Meta-Analysis Stroke*39, 2237–2248. https://doi.org/10.1161/STROKEAHA.107.509877

Djuricic, B. M., Paschen, W., Bosma, H. J., & Hossmann, K. A. (1983) Biochemical changes during graded brain ischemia in gerbils. Part 1. Global Biochemical Alterations. *Journal of the Neurological Sciences 58*, 25–36. https://doi.org/10.1016/0022-510X(83)90107-7

Dreher, W., Kuhn, B., Gyngell, M. L., Busch, E., Niendorf, T., Hossmann, K. A., & Leibfritz, D. (1998) Temporal and regional changes during focal ischemia in rat brain studied by proton spectroscopic imaging and quantitative diffusion NMR imaging. *Magnetic Resonance in Medicine 39*, 878–888. https://doi.org/10.1002/mrm.1910390605

Duarte, J. M. N., Lei, H., Mlynárik, V., & Gruetter, R. (2012) The neurochemical profile quantified by *in vivo* ^{1}H NMR spectroscopy. *NeuroImage 61*, 342–362. https://doi.org/10.1016/j.neuroimage.2011.12.038

Fisher, M., Prichard, J. W., & Warach, S. (1995) New magnetic resonance techniques for acute ischemic stroke. *JAMA 274*, 908–911. https://doi.org/10.1001/jama.1995.03530110070038

Gadian, D. G., Frackowiak, R. S., Crockard, H. A., Proctor, E., Allen, K., Williams, S. R., & Russell, R. W. (1987) Acute cerebral ischaemia: Concurrent changes in cerebral blood flow, energy metabolites, pH, and lactate measured with hydrogen clearance and 31P and 1H nuclear magnetic resonance spectroscopy. I. Methodology. *Journal of Cerebral Blood Flow and Metabolism 7*, 199–206. https://doi.org/10.1038/jcbfm.1987.45

Gruetter, R., & Tkac, I. (2000) Field mapping without reference scan using asymmetric echo-planar techniques. *Magnetic Resonance in Medicine*

43, 319–323. https://doi.org/10.1002/(SICI)1522-2594(20000 2)43:2<319:AID-MRM22>3.0.CO;2-1

Hilger, T., Niessen, F., Diedenhofen, M., Hossmann, K. A., & Hoehn, M. (2002) Magnetic resonance angiography of thromboembolic stroke in rats: Indicator of recanalization probability and tissue survival after recombinant tissue plasminogen activator treatment. *Journal of Cerebral Blood Flow and Metabolism 22*, 652–662. https://doi.org/10.1097/00004647-200206000-00003

Horikawa, Y., Naruse, S., Hirakawa, K., Tanaka, C., Nishikawa, H., & Watari, H. (1985) In vivo studies of energy metabolism in experimental cerebral ischemia using topical magnetic resonance. Changes in ^{31}P-nuclear magnetic resonance spectra compared with electroencephalograms and regional cerebral blood flow. *Journal of Cerebral Blood Flow and Metabolism 5*, 235–240. https://doi.org/10.1038/jcbfm.1985.30

Hossmann K. A. (1994) Viability thresholds and the penumbra of focal ischemia. *Annals of Neurology 36*, 557–565. https://doi.org/10.1002/ana.410360404

Kleihues, P., Hossmann, K. A., Pegg, A. E., Kobayashi, K., & Zimmermann, V. (1975) Resuscitation of the monkey brain after one hour complete ischemia. III. *Indications of Metabolic Recovery. Brain Research 95*, 61–73. https://doi.org/10.1016/0006-8993(75)90207-3

Kloiber, O., Miyazawa, T., Hoehn-Berlage, M., & Hossmann, K. A. (1993) Simultaneous ^{31}P NMR spectroscopy and laser Doppler flowmetry of rat brain during global ischemia and reperfusion. *NMR in Biomedicine6*, 144–152. https://doi.org/10.1002/nbm.1940060207

Lei, H., Berthet, C., Hirt, L., & Gruetter, R. (2009) Evolution of the neurochemical profile after transient focal cerebral ischemia in the mouse brain. *Journal of Cerebral Blood Flow and Metabolism 29*, 811–819. https://doi.org/10.1038/jcbfm.2009.8

Lei, H., Dirren, E., Poitry-Yamate, C., Schneider, B. L., Gruetter, R., & Aebischer, P. (2019) Evolution of the neurochemical profiles in the G93A-SOD1 mouse model of amyotrophic lateral sclerosis. *Journal of Cerebral Blood Flow and Metabolism 39*, 1283–1298. https://doi.org/10.1177/0271678X18756499

Mlynarik, V., Gambarota, G., Frenkel, H., & Gruetter, R. (2006) Localized short-echo-time proton MR spectroscopy with full signal-intensity acquisition. *Magnetic Resonance in Medicine 56*, 965–970. https://doi.org/10.1002/mrm.21043

Nagatomo, Y., Wick, M., Prielmeier, F., & Frahm, J. (1995) Dynamic monitoring of cerebral metabolites during and after transient global ischemia in rats by quantitative proton NMR spectroscopy in vivo. *NMR in Biomedicine8*, 265–270. https://doi.org/10.1002/nbm.1940080606

Nedergaard, M., Gjedde, A., & Diemer, N. H. (1986) Focal ischemia of the rat brain: Autoradiographic determination of cerebral glucose utilization, glucose content, and blood flow. *Journal of Cerebral Blood Flow and Metabolism 6*, 414–424. https://doi.org/10.1038/jcbfm.1986.74

Okada, Y., Shima, T., Nishida, M., & Kagawa, R. (1998) Magnetic resonance angiography visualization of four vessel (bilateral carotid and vertebral artery) occlusion–two case reports. *Neurologia medico-chirurgica (Tokyo)38*, 28–33. https://doi.org/10.2176/nmc.38.28

Öz, G., Alger, J. R., Barker, P. B., Bartha, R., Bizzi, A., Boesch, C., … Kauppinen, R. A. (2014) Clinical proton MR spectroscopy in central nervous system disorders. *Radiology 270*, 658–679. https://doi.org/10.1148/radiol.13130531

Perry, T. L., Hansen, S., & Gandham, S. S. (1981) Postmortem changes of amino compounds in human and rat brain. *Journal of Neurochemistry 36*, 406–412. https://doi.org/10.1111/j.1471-4159.1981.tb01608.x

Pulsinelli, W. A., & Brierley, J. B. (1979) A new model of bilateral hemispheric ischemia in the unanesthetized rat. *Stroke 10*, 267–272. https://doi.org/10.1161/01.STR.10.3.267

Reese, T., Bochelen, D., Sauter, A., Beckmann, N., & Rudin, M. (1999) Magnetic resonance angiography of the rat cerebrovascular system without the use of contrast agents. *NMR in Biomedicine12*, 189–196. https://doi.org/10.1002/(SICI)1099-1492(199906)12:4<189:AID-NBM557>3.0.CO;2-O

Sugio, K., Horigome, N., Sakaguchi, T., & Goto, M. (1988) A model of bilateral hemispheric ischemia–modified four-vessel occlusion in rats. *Stroke 19*, 922. https://doi.org/10.1161/str.19.7.922a

Taylor, J. M., Zhu, X. H., Zhang, Y., & Chen, W. (2015) Dynamic correlations between hemodynamic, metabolic, and neuronal responses to acute whole-brain ischemia. *NMR in Biomedicine 28*, 1357–1365. https://doi.org/10.1002/nbm.3408

Tkac, I., Henry, P. G., Andersen, P., Keene, C. D., Low, W. C., & Gruetter, R. (2004) Highly resolved in vivo 1H NMR spectroscopy of the mouse brain at 9.4 T. *Magnetic Resonance in Medicine 52*, 478–484.

Traystman R. J. (2003) Animal models of focal and global cerebral ischemia. *ILAR Journal 44*, 85–95. https://doi.org/10.1093/ilar.44.2.85

Xia, J., & Wishart, D. S. (2016) Using metaboanalyst 3.0 for comprehensive metabolomics data analysis. *Current protocols in bioinformatics 55*, 14 10 11–14 10 91.

Yamaguchi, M., Calvert, J. W., Kusaka, G., & Zhang, J. H. (2005) One-stage anterior approach for four-vessel occlusion in rat. *Stroke 36*, 2212–2214. https://doi.org/10.1161/01.STR.0000182238.08510.c5

SUPPORTING INFORMATION

Additional supporting information may be found online in the Supporting Information section.

How to cite this article: Lepore MG, Buscemi L, Hirt L, Lei H. Metabolic fingerprints discriminating severity of acute ischemia using in vivo high-field ^{1}H magnetic resonance spectroscopy. *J. Neurochem*. 2020;152:252–262. https://doi.org/10.1111/jnc.14922